

Transient Laminar-Film Condensation on a Vertical Plate

J. G. Reed,* F. M. Gerner,† and C. L. Tien‡
University of California, Berkeley, California

This work addresses the problem of transient, laminar-film condensation onto a vertical surface. It examines the behavior of the liquid film in response to changes in the temperature drop across the film or in the interfacial shear stress. Numerical solutions of the governing equations are compared with a simpler quasisteady analysis. The quasisteady analysis is adequate in many cases (e.g., atmospheric water). However, as the Jakob number or Jakob divided by Prandtl number approaches unity, the full equations and the quasisteady analysis yield significantly different predictions for heat transfer and mass flux during the transient. This reflects the increasing importance of accounting for the development of the temperature and velocity profiles.

Nomenclature

| | |
|--------------|--|
| C_p | = liquid specific heat |
| D^2 | = finite-difference form of the Laplacian operator |
| g | = gravitational acceleration |
| h_{fg} | = latent heat of vaporization |
| Ja | = Jakob number, $C_p \Delta T_o^+ / h_{fg}$ |
| k | = liquid thermal conductivity |
| L | = plate length |
| Pr | = liquid Prandtl number, ν/α |
| q | = interfacial heat flux |
| T | = temperature |
| t | = time |
| u | = streamwise velocity |
| v | = cross-stream velocity |
| x | = streamwise coordinate |
| y | = cross-stream coordinate |
| α | = liquid thermal diffusivity |
| Γ | = liquid mass flux per unit width of plate |
| δ | = film thickness |
| δ_N^+ | = film thickness at $x^+ = L$ using Nusselt theory |
| Δ | = difference or increment |
| μ | = liquid dynamic viscosity |
| ν | = liquid kinematic viscosity |
| ρ | = liquid density |
| τ | = interfacial shear stress |

Superscripts

| | |
|-----|------------------------|
| p | = time-step index |
| $+$ | = dimensional variable |

Subscripts

| | |
|------|--|
| m | = index in x direction |
| n | = index in y direction |
| ny | = number of grids in y direction |
| o | = initial state in transient analysis |
| r | = ramp input function for transient analysis |
| v | = vapor phase |
| w | = wall |

Introduction

THE present work addresses the problem of transient condensation of a laminar film onto a vertical surface with a counter-flowing vapor as shown in Fig. 1. The analysis looks at the time-dependent behavior of the liquid film in response to ramp changes in the temperature drop across the film or in the interfacial shear stress. While many analyses of laminar condensation on inclined surfaces have been performed,¹ only simplified analyses of the transient case have been done.^{2,3} The present analysis is the first to include the effects of inertia, convection, and interfacial shear stress under transient conditions.

The present analysis provides a quantitative assessment of the degree of approximation resulting from the use of quasisteady analyses which assume that the transient response is simply a sequence of steady-state solutions. This type of information is very useful in simplifying the analysis of the start-up or varying heat-load condition in gravity-assisted countercurrent condensing flows. For example, Reed and Tien⁴ use this information to make some major simplifications to a Dobran-type⁵ lumped-parameter two-phase closed thermosyphon model.

The simplest way to analyze transient, laminar-film condensation is to treat the velocity and temperature profiles as quasisteady and to neglect fluid inertia and convection. When this assumption is employed, the temperature profile is linear, and the velocity profile is parabolic. It has been shown¹ that the use of these profiles provides a very good approximation in steady-state systems when Ja and Ja/Pr are small relative to unity. Simple scaling analysis predicts that the same would be true in the transient case. In essence, for the quasisteady, no-convection profiles to be valid for the transient case, the time scales for cross-stream diffusion of momentum and energy must be short compared with the time scales governing changes in film thickness and mass flux. Quantitative assessment of the validity of this scaling argument is one of the key results of the present analysis.

In a previous analysis of transient, laminar-film condensation, Sparrow and Siegel² used a quasisteady approach to study vertical laminar-film condensation when there is a sudden drop in wall temperature. They used the method of characteristics to obtain a closed form solution. Chung³ performed a perturbation analysis to extend Sparrow and Siegel's work to include nonlinear temperature and nonparabolic velocity profiles. However, the coefficients in Chung's perturbation expansion, which depend on position along the plate and time, were not determined, so that actual temperature and velocity profiles cannot be obtained from his analysis, and the results are useful only for predicting trends. Neither of the two analyses include

Received April 13, 1987; presented as Paper 87-1534 at the AIAA 22nd Thermophysics Conference, Honolulu, HI, June 8-10, 1987; revision received Aug. 8, 1987. Copyright © American Institute of Aeronautics and Astronautics, Inc., 1987. All rights reserved.

*Currently Member of Technical Staff, General Research Corporation, Santa Barbara, CA. Associate Member AIAA.

†Professor, Department of Mechanical Engineering.

‡A. Martin Berlin Professor, Department of Mechanical Engineering. Fellow AIAA.

interfacial shear stress or quantitatively assess the effect of assuming linear temperature and parabolic velocity profiles.

The present model includes interfacial shear stress. Additionally, it incorporates the effects of inertia in the momentum equation and convection in the energy equation. It also includes a quantitative assessment of the inaccuracy of quasi-steady analyses which assume that the transient response is simply a sequence of Nusselt-type (i.e., no convective or storage terms) steady-state solutions. In the following sections the governing equations will be presented and the finite-difference formulation used to solve these equations will be discussed. Graphical results illustrate the liquid film's response to transient changes in interface temperature and interfacial shear stress for both the full analysis and a simpler quasisteady approach.

Mathematical Formulation

The differential equations governing transient condensation onto a vertical plate, of a laminar film with constant properties, using the geometry defined in Fig. 1, are the following

$$\frac{\partial u^+}{\partial x^+} + \frac{\partial v^+}{\partial y^+} = 0 \quad (1)$$

$$\left[\frac{\partial u^+}{\partial t^+} + u^+ \frac{\partial u^+}{\partial x^+} + v^+ \frac{\partial u^+}{\partial y^+} \right] = g + v \frac{\partial^2 u^+}{\partial y^{+2}} \quad (2)$$

and

$$\left[\frac{\partial T^+}{\partial t^+} + u^+ \frac{\partial T^+}{\partial x^+} + v^+ \frac{\partial T^+}{\partial y^+} \right] = \alpha \frac{\partial^2 T^+}{\partial y^{+2}} \quad (3)$$

where the bracketed terms are not included in a quasisteady analysis. Standard boundary-layer assumptions have been invoked to arrive at these equations for conservation of mass, momentum, and energy. The only additional assumption is that there is no imposed pressure gradient in the streamwise direction. Since, for almost all applications, the film is thin relative to the length of the plate, axial conduction is negligible relative to cross-stream conduction. Of course, for certain ranges of the dimensionless parameters, convection may also be negligible. But for all cases considered, these equations include the dominant terms.

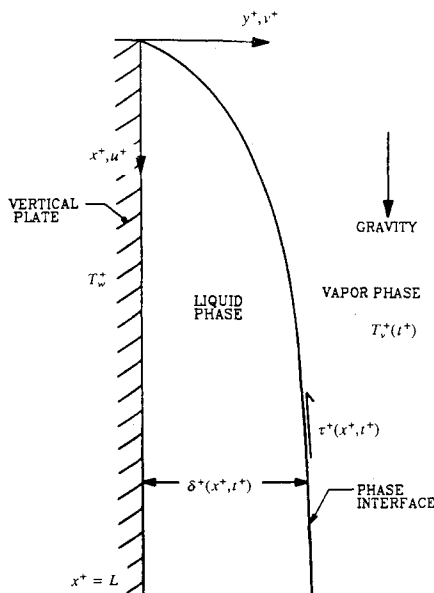


Fig. 1 Transient laminar-film condensation on a vertical flat plate.

The boundary conditions employed in this analysis are

$$u^+(x^+, 0, t^+) = v^+(x^+, 0, t^+) = 0 \quad (4a)$$

$$\mu \frac{\partial u^+(x^+, \delta^+, t^+)}{\partial y^+} = \tau^+(x^+, t^+) \quad (4b)$$

$$T^+(x^+, 0, t^+) = T_w^+ = \text{constant} \quad (4c)$$

and

$$T^+(x^+, \delta^+, t^+) = T_v^+(t^+) \quad (4d)$$

Equation (4a) represents the no-slip condition at the wall, Eq. (4b) is a force balance at the vapor-liquid interface, and Eqs. (4c) and (4d) are boundary conditions on the temperature. The functions $\tau^+(x^+, t^+)$ and $T_v^+(t^+)$ are inputs representing the transient changes in the vapor.

The equation for continuity of mass at the interface is

$$\rho \frac{\partial \delta^+}{\partial t^+} = \frac{q^+}{h_{fg}} - \frac{\partial \Gamma^+}{\partial x^+} \quad (5)$$

where q^+ is the heat flux at the interface and Γ^+ is the mass flux of the liquid film per unit width of the plate. This equation represents a balance between the rate of change of film thickness, interfacial heat flux and mass rate of condensation. The initial velocity and temperature distributions for the transient solution are specified using a steady-state solution of the above system for the boundary conditions which apply at the start of the transient (for the quasisteady case this is a Nusselt-type solution).

The governing equations and boundary conditions can be made dimensionless by introducing the following variables:

$$\begin{aligned} x &= \frac{x^+}{L}, \quad y = \frac{y^+}{\delta_N^+}, \quad t = t^+ \left[\frac{g \delta_N^{+2}}{\nu L} \right] \\ \delta &= \frac{\delta^+}{\delta_N^+}, \quad u = \frac{u^+}{(g \delta_N^{+2} / \nu)}, \quad v = \frac{v^+}{(g \delta_N^{+2} / \nu L)} \\ \Gamma &= \frac{\Gamma^+}{(\rho g \delta_N^{+3} / \nu)}, \quad q = \frac{q^+ \delta_N^+}{k \Delta T_o^+}, \quad \tau = \frac{\tau^+}{\rho g \delta_N^+} \\ T &= \frac{T^+ - T_w^+}{\Delta T_o^+}, \quad \text{Ja} = \frac{C_p \Delta T_o^+}{h_{fg}}, \quad \text{Pr} = \frac{\nu}{\alpha} \end{aligned} \quad (6)$$

In the above definitions, ΔT_o^+ is the initial temperature difference across the liquid film and δ_N^+ is the film thickness at $x^+ = L$ calculated from Nusselt theory¹ for a temperature difference of ΔT_o^+ ($\delta_N^+ = [4 (\text{Ja}/\text{Pr}) (\nu^2 L/g)]^{1/4}$). It should also be noted that the time scale arises from balancing the terms in Eq. (5). This time scale is identical to that used in the analysis of Sparrow and Siegel.² It should be noted that it is implicit in this scaling that cross-stream diffusion of energy occurs over a time scale faster than that governing film growth. When this is true, steady state will be reached when the dimensionless time is of the order of unity. One purpose of the present analysis is to investigate the conditions under which this scaling is valid.

Using the above definitions, the dimensionless governing equations become

$$\frac{\partial u}{\partial x} + \frac{\partial v}{\partial y} = 0 \quad (7)$$

$$4 \frac{\text{Ja}}{\text{Pr}} \left[\frac{\partial u}{\partial t} + u \frac{\partial u}{\partial x} + v \frac{\partial u}{\partial y} \right] = 1 + \frac{\partial^2 u}{\partial y^2} \quad (8)$$

and

$$4 \text{Ja} \left[\frac{\partial T}{\partial t} + u \frac{\partial T}{\partial x} + v \frac{\partial T}{\partial y} \right] = \frac{\partial^2 T}{\partial y^2} \quad (9)$$

The dimensionless boundary conditions are

$$u(x, 0, t) = v(x, 0, t) = 0 \quad (10a)$$

$$\frac{\partial u(x, \delta, t)}{\partial y} = \tau(x, t) \quad (10b)$$

$$T(x, 0, t) = 0 \quad (10c)$$

and

$$T(x, \delta, t) = T_v(t) \quad (10d)$$

The equation for continuity of mass at the interface becomes

$$\frac{\partial \delta}{\partial t} = \frac{q}{4} - \frac{\partial \Gamma}{\partial x} \quad (11)$$

The transient inputs chosen for this analysis are

$$\tau(x, t) = \begin{cases} \frac{t}{\Delta t_r} \frac{(x)^{1/4}}{4} & t \leq \Delta t_r \\ \frac{(x)^{1/4}}{4} & t > \Delta t_r \end{cases} \quad (12a)$$

and

$$T_v(t) = \begin{cases} 1 + \frac{1}{2} \frac{t}{\Delta t_r} & t \leq \Delta t_r \\ 1.5 & t > \Delta t_r \end{cases} \quad (12b)$$

where Δt_r is the dimensionless ramp time, chosen to be 0.1 for our results. The interfacial shear stress function above corresponds to a ramp between zero and a value equal to one-fourth of the initial weight of the film, in the grid zone at x , divided by Δx . The vapor temperature input was chosen to give a reasonable change in film thickness between the initial and final states. These input functions would be representative of a counter-current vapor flow of increasing flow rate and temperature such as would occur in a reflux condensation system under increasing heat load.

Method of Solution

Since the system of Eqs. (7–12) has no known analytical solution, a numerical solution has been performed. In order to account for the fact that the film thickness varies with axial distance a control-volume or lumped-capacity method⁶ is used to express the equations in finite-difference form. In the equations below, the superscript indicates the time step; $p+1$ refers to the current time step and p indicates the previous time step. The subscript m, n means that the variable is evaluated at the m th grid point in the x -direction and the n th grid point in the y direction. The variables Δx , Δy_m^p , and Δt are the grid spacing in the x and y directions and the time step respectively, and the operator D^2 signifies the difference form of the Laplacian (a fully implicit calculation of the Laplacian is used). Note that, because of the changing film thickness, the grid spacing in the y direction is a function of streamwise location and time. The difference equations corresponding to Eqs. (7–11) are

$$\frac{u_{m,n}^{p+1} - u_{m-1,n}^{p+1} \left(\frac{\Delta y_{m-1}^p}{\Delta y_m^p} \right)}{\Delta x} + \frac{v_{m,n}^{p+1} - v_{m,n-1}^{p+1}}{\Delta y_m^p} = 0 \quad (13)$$

$$4 \frac{\text{Ja}}{\text{Pr}} \left[\frac{u_{m,n}^{p+1} - u_{m,n}^p}{\Delta t} + \frac{(u_{m,n}^p)^2 \Delta y_m^p - (u_{m-1,n}^p)^2 \Delta y_{m-1}^p}{\Delta x \Delta y_m^p} + \frac{v_{m,n}^p u_{m,n}^p - v_{m,n-1}^p u_{m,n-1}^p}{\Delta y_m^p} \right] = 1 + D^2(u_{m,n}^{p+1}) \quad (14)$$

$$4 \text{Ja} \left[\frac{T_{m,n}^{p+1} - T_{m,n}^p}{\Delta t} + \frac{u_{m,n}^p T_{m,n}^p \Delta y_m^p - u_{m-1,n}^p T_{m-1,n}^p \Delta y_{m-1}^p}{\Delta x \Delta y_m^p} + \frac{v_{m,n}^p T_{m,n}^p - v_{m,n-1}^p T_{m,n-1}^p}{\Delta y_m^p} \right] = D^2(T_{m,n}^{p+1}) \quad (15)$$

and

$$\frac{\delta_m^{p+1} - \delta_m^p}{\Delta t} = \frac{q_m^p + q_m^{p+1} + q_{m-1}^p + q_{m-1}^{p+1}}{16} - \frac{(\Gamma_m^p - \Gamma_{m-1}^p) + (\Gamma_m^{p+1} - \Gamma_{m-1}^{p+1})}{2 \Delta x} \quad (16)$$

As before, the bracketed terms are not included in a quasi-steady analysis. The difference forms of the boundary conditions are obtained from Eq. (10) as

$$u_{m,1}^{p+1} = v_{m,1}^{p+1} = 0 \quad (17a)$$

$$\frac{u_{m,ny}^{p+1} - u_{m,ny-1}^{p+1}}{\Delta y_m^p} = \tau_m^{p+1} \quad (17b)$$

$$T_{m,1}^{p+1} = 0 \quad (17c)$$

and

$$T_{m,ny}^{p+1} = T_v((p+1) \Delta t) \quad (17d)$$

The initial steady-state solution is found using the transient code with constant boundary conditions and the classical Nusselt solution¹ as an initial guess. As the boundary conditions are ramped finite-difference equations [Eqs. (14) and (15)] are solved at each time-step using a tridiagonal matrix inversion technique. The film thickness is then updated using Eq. (16). Note that since q^{p+1} and Γ^{p+1} are known, calculation of δ^{p+1} is an explicit integration in time.

During transient calculations, the grid must be adjusted as the solution proceeds because of the changing film thickness. At the end of each time step, the film thickness at each station in the streamwise direction is updated using Eq. (16). Since the heat flux is indeterminate at $x = 0$ (because the film thickness is zero there), the average heat flux in the first grid element is taken as $1.333q_1^{p+1}$ which is a result derived from Nusselt theory.¹ For purposes of evaluating the mass fluxes and interfacial heat flux for use in Eq. (16), it is assumed that the velocity and temperature profiles, in terms of (y/δ) , remain unchanged across the time step. Although this is not strictly correct, in the present analysis, the time step is kept small enough that the change in film thickness during each time step is so small that the difference in velocity and temperature profiles calculated using the original and updated grids is negligible. A more physically correct procedure might be to use an iterative predictor-corrector method wherein the new film thickness is estimated using the velocity and temperature profiles calculated with the old grid, and the estimated film thicknesses are then used to recalculate the velocity and temperature profiles which are then used to obtain a new estimate of the updated film thickness at each location. In the present case, the need for an iterative approach is avoided by employing small time steps.

At the leading edge of the plate, the film thickness calculation is complicated by the fact that the thermal resistance of the film, the mass of the film, and the heat capacity of the film are all very small. In order to achieve stability with a reasonable

time step in the calculation of the position of the interface, which is essentially an explicit integration in time, special consideration must be given to the grid increment in the x direction. Although the stability of the calculation is controlled by the condensation rate that primarily depends on cross-stream transport of energy, the grid spacing in the x direction is important because of the effect of the convective terms on stability and because the grid size in the x direction determines the magnitude of the film thickness at the first grid point in the mesh. Specifically, the grid increment must be large enough for the film thickness at the first grid point to be sufficiently large to ensure that the change in film thickness during a single time step is small relative to the current film thickness. No formal criterion for stability of the calculation has been derived (this would be extremely difficult), and the grid increments and time step used in the calculations presented below were determined by specifying the resolution of the profiles in the y direction and then choosing the time step and grid size in the x direction by trial and error to obtain a stable calculation with reasonable resolution in the x direction with a time step that was not prohibitively small. Note that since the same grid is used for both momentum and energy, its size is determined by the more restrictive of the two equations. In order to avoid instability of the other equation, small time steps are taken. If the time step is increased, for a given grid size, oscillatory behavior will appear in the calculated results as the point of instability is approached. In the results presented below, $\Delta x = 0.033$, $\Delta y / \delta = 0.05$, $\Delta \tau = 0.1$ and $\Delta t = 10^{-3}$.

Results

In order to check the validity of quasisteady analysis for very small Jakob and Jakob divided by Prandtl numbers, numerical calculations, including convective and inertial terms, were performed for Ja and Ja/Pr both equal to 10^{-3} . Velocities, temperatures, and film thicknesses were almost identical to those predicted by a quasisteady analysis for all times. This is not very surprising since Ja and Ja/Pr measure the sizes of the time scales for diffusion of energy and momentum relative to the film residence time. This merely confirms that if cross-stream diffusion occurs very rapidly, convective terms are insignificant.

Of course for most realistic applications Ja and Ja/Pr are much larger. In order to assess whether the small parameter quasisteady approach is valid for practical applications, calculations were performed for $Ja = 0.108$ and $Ja/Pr = 0.042$, which is representative for atmospheric water with an average temperature of 70°C and initially a 60°C temperature drop across the liquid film. These results are presented in Figs. 2 through 5.

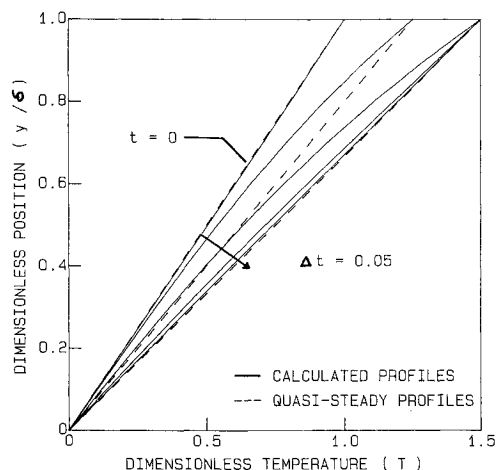


Fig. 2 Developing temperature profiles, $Ja = 0.108$, $Ja/Pr = 0.042$.

Figures 2 and 3 show the development of the temperature and velocity profiles at $x = 1.0$, where the film thickness is at its maximum, meaning that the profiles shown develop more slowly than those at smaller values of x . The time increment between the successive profiles shown in the figures is $\Delta t = 0.05$ (0.048 s) and, as can be seen in the figures, the calculated and quasisteady profiles show good agreement for $t > 0.2$ (0.19 s). It should be noted that the solid and dashed curves do not match exactly at either time zero nor at the new steady state. This is because the steady state calculated for the quasisteady case does not include convective or inertial terms, while the full

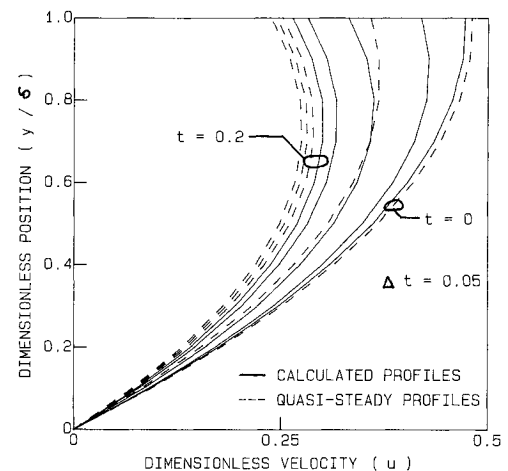


Fig. 3 Developing velocity profiles, $Ja = 0.108$, $Ja/Pr = 0.042$.

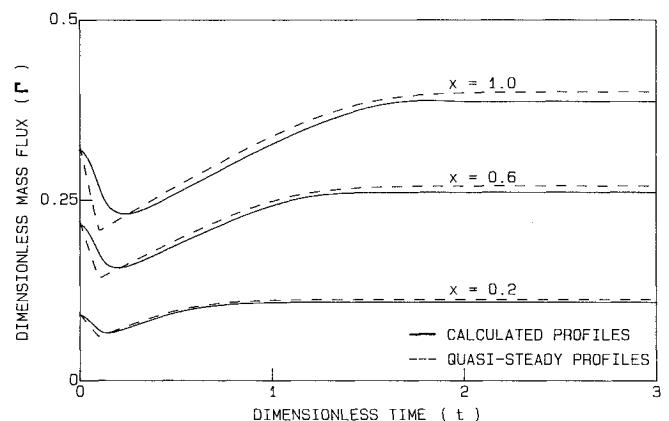


Fig. 4 Mass flux vs time, $Ja = 0.108$, $Ja/Pr = 0.042$.

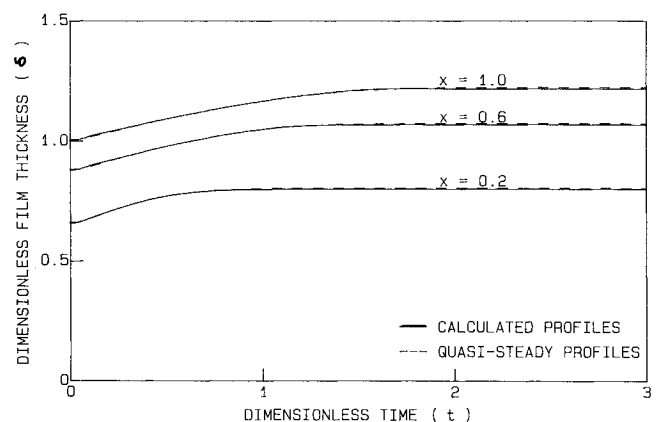


Fig. 5 Film thickness vs time, $Ja = 0.108$, $Ja/Pr = 0.042$.

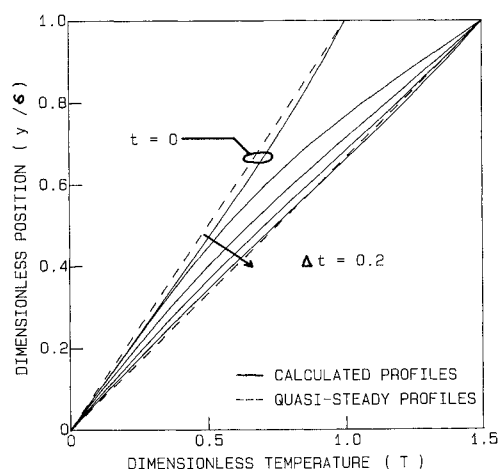


Fig. 6 Developing temperature profiles, $Ja = 1$, $Ja/Pr = 10^{-3}$.

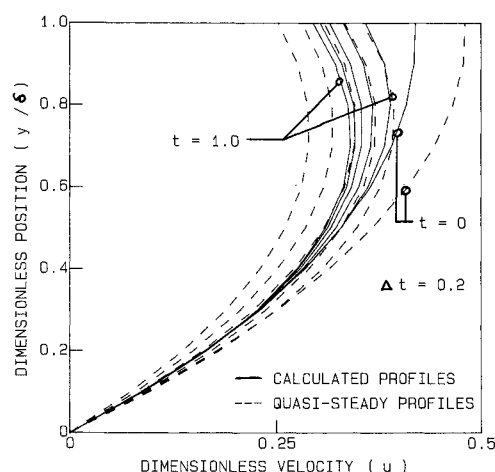


Fig. 7 Developing velocity profiles, $Ja = 10^{-3}$, $Ja/Pr = 1$.

calculation does. The fact that the profiles develop rapidly in comparison to typical rise times for film thickness and mass flux provides an indication that neglecting the time required for the profiles to develop will have little influence on the transient calculations for film thickness and liquid-film mass flux. This is verified in Figs. 4 and 5, which show graphical comparisons of the dimensionless mass flux and dimensionless film thickness at various streamwise locations obtained using the calculated and quasisteady velocity and temperature profiles. The difference in the values obtained by the two methods is very small at all times during the transient except in the dimensionless mass flux calculations for the very early-time regime, $t < 0.2$, where the deviation between the calculations displays a maximum value of about 20% of the larger value. The difference in the calculated dimensionless mass flux is due to the fact that, for such a rapid increase in interfacial shear, the acceleration of the film near the interface is significant, and the storage terms in the momentum equation are not negligible. On the other hand, the film thickness predictions of the two methods of calculation show very little deviation. This is because, although a rapid increase in vapor temperature causes a rapid increase in energy transport across the film, the large latent heat of the working fluid has a mitigating effect on the rate of increase in film thickness. In addition, even in the calculation using quasisteady profiles, storage terms are included in the film thickness calculation, although in an approximate way. Even the 20% deviation seen in the dimensionless mass flux calculations is rather small when it is considered that the transient inputs are nearly step functions.

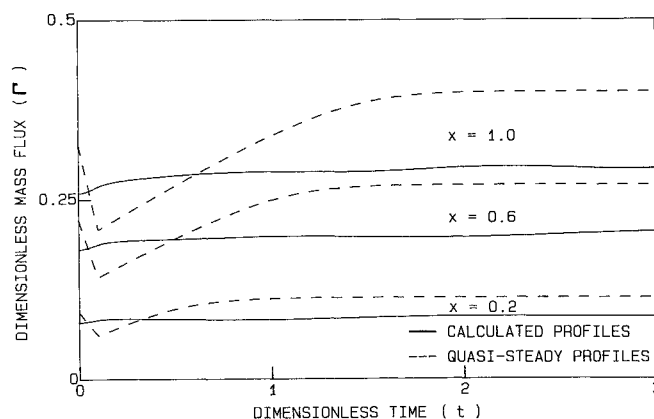


Fig. 8 Mass flux vs time, $Ja = 1$, $Ja/Pr = 1$.

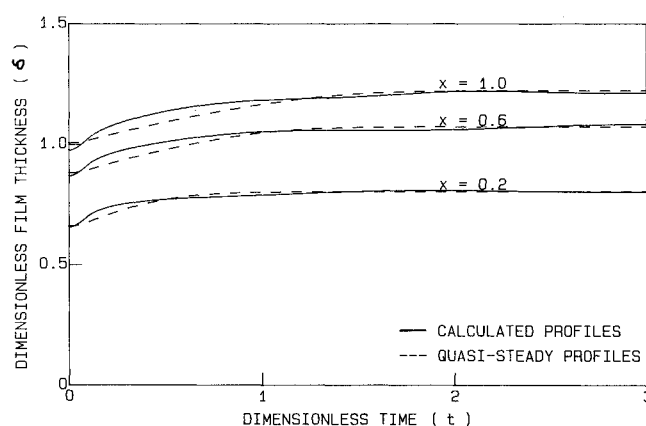


Fig. 9 Film thickness vs time, $Ja = 1$, $Ja/Pr = 1$.

Since the quasisteady approach seems to work well for atmospheric water, the next logical question is, when does this method fail? In order to answer this question the following cases were examined:

| Case | Ja | Ja/Pr |
|------|-----------|-----------|
| I | 1.0 | 1.0 |
| II | 1.0 | 10^{-3} |
| III | 10^{-3} | 1.0 |

The large Ja number cases would correspond, for example, to working fluids with relatively high heat capacity or relatively low heat of vaporization. They can also correspond to cases with large temperature drops across the film. The large Ja/Pr cases can result from the above causes or from a small value of Pr . Some graphical results for these cases are shown in Figs. 6-9.

As expected, for large Jakob numbers the temperature profiles are no longer linear. Figure 6 shows the temperature profile at $x = 1$ for case II (case I is very similar). The time increment between successive profiles is $\Delta t = 0.2$. It is seen that the time for the temperature to develop ($t > 1.0$) is much greater than for atmospheric water ($t > 0.2$). From the slopes of the solid curves it can be seen that initially much more heat is transferred at the interface than at the wall. The rest of the energy is convected downstream. For case III, although the Ja/Pr number is large, the small Ja number results in a quasisteady temperature profile.

As case III, shown in Fig. 7, demonstrates, when the Ja/Pr number is large, the velocity profile is very slow in developing (case I shows similar results). It requires $t > 1.0$, as compared

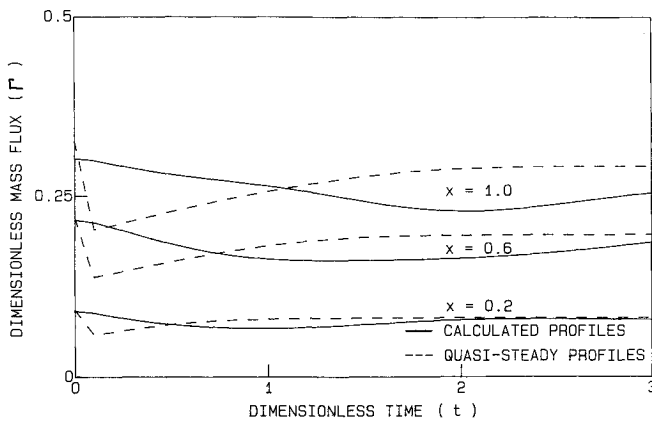


Fig. 10 Mass flux vs time, $Ja = 10^{-3}$, $Ja/Pr = 1$, $T_i(t) = 1$.

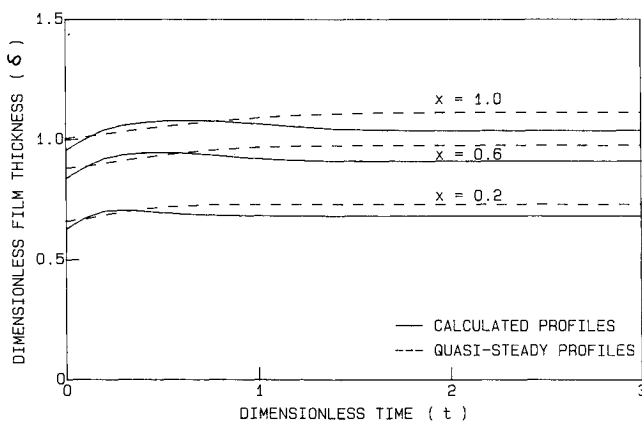


Fig. 11 Film thickness vs time, $Ja = 1$, $Ja/Pr = 10^{-3}$, $\tau(x,t) = 0$.

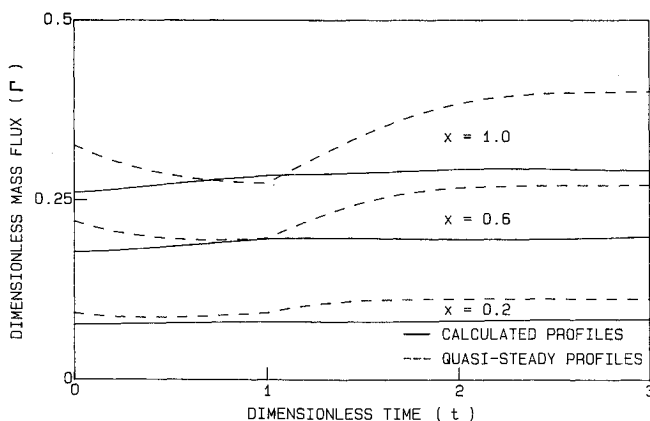


Fig. 12 Mass flux vs time, $Ja = 1$, $Ja/Pr = 1$, $\Delta t_r = 1$.

to $t > 0.2$ for atmospheric water. Since

$$4 Ja/Pr = \frac{\delta_N^{+3} g \delta_N^+}{\nu^2 L}$$

which is the product of the Galileo number and film aspect ratio, another interpretation is that a high aspect ratio delays development of the velocity profile. To summarize, the Ja number determines the shape and development of the temperature profile, while the Ja/Pr number determines the shape and the development of the velocity profile.

Figures 8 and 9 show graphical comparisons of the dimensionless mass flux and the dimensionless film thickness at vari-

ous streamwise locations, for $Ja = 1.0$ and $Ja/Pr = 1.0$. Figure 8 shows that the behavior of the mass-flux curves for the quasisteady and full calculations is significantly different. The quasisteady calculations predict initial decreases in mass flux because the increase in interfacial shear is immediately transmitted through the entire film while the full calculations account for the finite diffusion time. This effect can perhaps be seen more clearly by ramping only the interfacial shear stress. Figure 10 shows the mass flux as a function of time for $Ja = 10^{-3}$, $Ja/Pr = 1$, and $T_i = 1$ (i.e., the interfacial temperature is not ramped). In both cases, the interfacial shear stress inhibits the flow. The quasisteady analysis predicts this effect will be felt immediately, while the full calculation accounts for the time required for momentum to diffuse across the film. Thus the use of quasisteady profiles appears to breakdown for Ja and Ja/Pr of order 1.0. In Fig. 9 the absolute error in film thickness is not large because of the relatively small change in film thickness between the two steady states (this is because film thickness increases as the temperature difference to the one-quarter power). However, the difference in rise time between the quasisteady and full transient calculations is significant. As Fig. 11 for $Ja = 1$, $Ja/Pr = 10^{-3}$, and $\tau = 0$ (i.e., no ramp in interfacial shear stress) shows the quasisteady temperature profile's rapid development causes the film thickness to increase monotonically to a new steady state. For the full calculation, however, the temperature profile develops more slowly. As evidenced by nonlinear temperature profiles, there is downstream convection which tends to increase the velocity and film thickness during the early transient. The film thickness increases rapidly and overshoots before settling down to a new steady state. Velocity, temperature, and mass flux development tend to support these conclusions.

Before presenting our conclusions, it is instructive to review the generality of our results. Both the transient changes in vapor temperature and interfacial shear stress were quite significant. For less drastic changes, the quasisteady approach should be even better. The ramp time for vapor temperature and interfacial shear stress, however, restricts the generality of our results. In order to show that our results are general, we ran the case of $Ja = 1$, $Ja/Pr = 1$ with a dimensionless ramp time, Δt_r , of 0.01 (all previous results were with $\Delta t_r = 0.1$). Velocity and temperature profiles, film thickness and mass flux calculations were practically identical to the $\Delta t_r = 0.1$ case, except for very early times. For much larger ramp times (larger than $\Delta t_r = 0.1$) the quasisteady analysis works better. Figure 12 demonstrates this for $Ja = 1$, $Ja/Pr = 1$, and $\Delta t_r = 1$. In this case the time rise for the inputs is of the same order as the rise time for film thickness, and the quasisteady approach works better (see Fig. 8 for comparison). Of course for such large Ja and Ja/Pr the "steady-state" convective effect is still very important.

Conclusions

It has been found that a simple quasisteady analysis adequately predicts the transient response of a condensing liquid water film for atmospheric conditions. Even for Jakob and Jakob divided by Prandtl number of unity, the quasisteady approach is able to predict film thickness accurately, although the transient rise time is not well predicted. One reason for this is that the overall change in film thickness is much smaller than the change in temperature drop across the film. High Jakob and Jakob divided by Prandtl numbers slow the development of the temperature and velocity profiles; therefore quasisteady analyses overpredict the heat transfer at the wall and underpredict the mass flux during the early stages of the transient. Based on the results obtained in this study, it is not required that Ja and Ja/Pr be much smaller than one to justify the quasisteady approach (for Ja and Ja/Pr less than 0.1 the quasisteady approach is very good). It is merely required that they be less than the order of unity. This parallels results for steady-state analyses which show that neglecting convection and inertia in the

liquid film is well justified up to Jakob and Jakob divided by Prandtl numbers of order one.

References

¹Collier, J. G., *Convective Boiling and Condensation*, 2nd ed., 1981, McGraw-Hill, New York, pp. 328–335.

²Sparrow, E. M. and Siegel, R., "Transient Film Condensation," *Journal of Applied Mechanics*, Vol. 26, 1959, pp. 120–121.

³Chung, P. M., "Unsteady Laminar Film Condensation on a Verti-

cal Plate," *Journal of Heat Transfer*, Vol. 85, 1963, pp. 63–70.

⁴Reed, J. G. and Tien, C. L., "Modeling of the Two-Phase Closed Thermosyphon," *Journal of Heat Transfer*, Vol. 109, 1987, pp. 722–730.

⁵Dobran, F., "Stability Thresholds of a Closed Two-Phase Thermosyphon," *Fifth International Heat Pipe Conference*, Vol. 4, 1984, Tsukuba, Japan, pp. 64–70.

⁶Holman, J. P., *Heat Transfer*, 6th ed., 1986, McGraw-Hill, New York, pp. 166–170.

From the AIAA Progress in Astronautics and Aeronautics Series

THERMOPHYSICS OF ATMOSPHERIC ENTRY—v. 82

Edited by T.E. Horton, The University of Mississippi

Thermophysics denotes a blend of the classical sciences of heat transfer, fluid mechanics, materials, and electromagnetic theory with the microphysical sciences of solid state, physical optics, and atomic and molecular dynamics. All of these sciences are involved and interconnected in the problem of entry into a planetary atmosphere at spaceflight speeds. At such high speeds, the adjacent atmospheric gas is not only compressed and heated to very high temperatures, but strongly reactive, highly radiative, and electronically conductive as well. At the same time, as a consequence of the intense surface heating, the temperature of the material of the entry vehicle is raised to a degree such that material ablation and chemical reaction become prominent. This volume deals with all of these processes, as they are viewed by the research and engineering community today, not only at the detailed physical and chemical level, but also at the system engineering and design level, for spacecraft intended for entry into the atmosphere of the earth and those of other planets. The twenty-two papers in this volume represent some of the most important recent advances in this field, contributed by highly qualified research scientists and engineers with intimate knowledge of current problems.

Published in 1982, 521 pp., 6 × 9, illus., \$29.95 Mem., \$59.95 List

TO ORDER WRITE: Publications Dept., AIAA, 370 L'Enfant Promenade, SW, Washington, DC 20024